where $\eta = (3/2\pi) \int_0^\infty dz\, z^2(e^z + 1)^{-1} \sim 0.86$. The additional factor k_BT reflects the linear density of states at the nodes (*3*). Thus, the QP current in the clean *d*-wave superconductor varies as T^2 in the limit $T \rightarrow 0$, which is consistent with Fig. 4B. Equation 2 provides a good fit to the measured κ^{2D} with a relaxation time $1/\Gamma = 0.38$ ps.

These comparisons show that it is reasonable to identify the total field-induced change $\Delta\kappa(H_k, T)$ with the value of κ_e in zero field. However, the inference that $\kappa_e = 0$ in the plateau region presents a challenge to our understanding of the QP state. The simplest way to have $\kappa_e = 0$ is to assume that the QP density n_{QP} vanishes (above H_k). This could arise from a gap Δ_H that opens gradually with field, leading to an exponential decay, namely $n_{QP} \sim \exp(-\Delta_H/k_BT)$ (Δ_H is distinct from the superconducting gap).

However, the observed behavior of κ is incompatible with an exponential decrease in κ_e. As discussed above, the break at H_k is nonanalytic. It is strongly suggestive of a phase transition between distinct states of the condensate: A large gap appears abruptly at the field H_k. A number of possibilities come to mind. One proposal (*13*) is that the field may induce an abrupt change of gap parameter symmetry, from a simple *d* wave to a complex order parameter (such as $d_{x^2-y^2} + id_{xy}$ or $d_{x^2-y^2} + is$) that reflects the breaking of time-reversal invariance in the field. A complex gap parameter implies that the superconducting gap is non-zero everywhere on the FS. In the new phase, the removal of the nodes abruptly drives the QP population, as well as κ_e, to zero. This scenario, if valid, implies that the superconducting state in the cuprates may have other unexpected properties.

We have also repeated the measurements with **H** in-plane and perpendicular to $-\nabla T$. The behavior is qualitatively different from the behavior reported here and is much weaker in field sensitivity. This difference implies that the changes at H_k are predominantly an orbital effect of the field (as opposed to the Zeeman term involving the spins).

Finally, we comment on the constraint on the phonon current. The condition $\partial\kappa_{ph}/\partial H = 0$ means that vortices in Bi 2212 do not scatter phonons above H_k, despite the rather long phonon mean free path ℓ_{ph} (*14*). Insofar as the behavior at H_k is associated with the QPs, we may extend this conclusion to fields below H_k as well. The absence of phonon scattering by vortices stands in striking contrast to the situation in classical Bardeen-Cooper-Schrieffer superconductors (*15*), where vortices are strong scatterers of phonons.

REFERENCES AND NOTES

1. C. C. Tsuei *et al.*, *Phys. Rev. Lett.* **73**, 593 (1994).
2. D. A. Bonn *et al.*, *ibid.* **68**, 2390 (1992); D. A. Bonn *et al.*, *Phys. Rev. B* **47**, 11314 (1993).
3. K. A. Moler *et al.*, *Phys. Rev. Lett* **73**, 2744 (1994).
4. A. Jezowski *et al.*, *Phys. Lett. A* **122**, 431 (1987); C. Uher and A. B. Kaiser, *Phys. Rev. B* **36**, 5680 (1987).
5. S. Hagen, Z. Z. Wang, N. P. Ong, *Phys. Rev. B* **40**, 9389 (1989).
6. R. C. Yu, M. B. Salamon, J. P. Lu, W. C. Lee, *Phys. Rev. Lett.* **68**, 1431 (1992).
7. K. Krishana, J. M. Harris, N. P. Ong, *ibid.* **75**, 3529 (1995).
8. At our highest resolution, several background effects are observable. The most significant arises from the weak MR of the thin-film resistors, which is about one part in 10^3 at 14 T. This produces an extraneous, slowly rising background (versus *H*) when the voltage across the heater is used to monitor the heater current at the sample. The measurements are not affected by a putative field gradient between the sample and the reference. With our field homogeneity (one part in 10^4 over 1 mm), the maximum thermocouple distortion in a field of 1 T is 100 times smaller than our resolution. The two crystals investigated were cut from a boule grown by the traveling-solvent floating-zone technique. Optical microscopy showed the crystal to be single-domained (the structural modulations all lie in one direction).
9. E. Zeldov *et al.*, *Nature* **375**, 373 (1995).
10. J. Bardeen, G. Rickayzen, L. Tewordt, *Phys. Rev.* **113**, 982 (1959).
11. L. P. Kadanoff and P. C. Martin, *ibid.*, **124**, 670 (1961).
12. We are grateful to R. B. Laughlin for help in computing κ_e.
13. P. W. Anderson and F. D. M. Haldane, private communication.
14. From the heat capacity c_v at low *T* and the relation $\kappa_{ph} = c_v\ell_{ph}v_s/3$, we obtain a lower bound for ℓ_{ph} of 1200 Å at 10 K (the sound velocity $v_s < 5 \times 10^3$ m/s). Thus, scattering of phonons by vortex cores should be easily observed (the vortex lattice spacing is 450 Å at 1 T). $c_v \sim 10.8$ mJ/cm^3 K at 10 K [see A. Junod *et al.*, *Physica C* **162–164**, 480 (1989)].
15. W. F. Vinen, E. M. Forgan, C. E. Gough, M. J. Hood, *Physica* **55**, 94 (1971).
16. We have benefitted from discussions with P. W. Anderson, H. Fukuyama, F. D. M. Haldane, R. B. Laughlin, and P. A. Lee. Research at Princeton is supported by the U.S. Office of Naval Research (contract N00014-90-J-1013) and NSF (DMR 94-00362). Q.L. was supported by the U.S. Department of Energy, Division of Materials Science, contract DE-AC02-76CH00016.

18 March 1997; accepted 5 May 1997

Nuclear Spectroscopy in Single Quantum Dots: Nanoscopic Raman Scattering and Nuclear Magnetic Resonance

D. Gammon,* S. W. Brown,† E. S. Snow, T. A. Kennedy, D. S. Katzer, D. Park

Resonant Raman and nuclear magnetic resonance spectroscopies from single gallium arsenide quantum dots are demonstrated. The nuclei were probed through changes in the optical spectra of the quantum dot exciton arising from exciton-nuclear interactions. This approach allowed the application of optical spectroscopy with its extremely high sensitivity and selectivity. The experiments had a lateral spatial resolution of about 10 nanometers and probe a volume that was five orders of magnitude smaller than that of previous semiconductor nuclear spectroscopic studies.

Semiconductors are typically modeled in terms of almost independent electronic and nuclear systems with coupling through relatively weak electron-nuclear interactions. The electronic system can be studied at optical frequencies through sensitive optical spectroscopies with tunable lasers and highly sensitive detectors. Recently there has been significant progress in the spectroscopic study of very small semiconductor samples, culminating with the detailed study of individual quantum dots (QDs), which are solid-state crystalline structures so small that their electronic wave function is completely localized and their energy spectrum is fully quantized (*1*–*6*). It has been shown that the optical linewidths of single QDs are orders of magnitude narrower than those observed in ensemble measurements. In fact, the linewidths can approach the natural linewidths expected from radiative lifetimes (*3*). With such narrow lines in the optical spectra, single QD spectroscopy has led, for example, to the direct observation of fine structure (*4*), hyperfine shifts (*5*), and spectral wandering (*6*). Single QD spectroscopy has followed the earlier examples of atomic and, especially, single molecule spectroscopies (*7*). To date, however, only the electronic spectra of single QDs have been measured. Here we report spectroscopic measurements of the nuclear system in a single QD. The capability to do nuclear spectroscopy on a scale of 10 nm in single QDs could provide sensitive measurements of local strain and chemical composition, issues of great importance for semiconductor nanostructures.

Naval Research Laboratory, Washington, DC 20375–5347, USA.

*To whom correspondence should be addressed. E-mail: gammon@bloch.nrl.navy.mil

†Present address: National Institute of Standards and Technology, Gaithersburg, MD 20899, USA.

Here we will consider the bound electron-hole pair known as an exciton. An exciton in a QD interacts with the nuclei through either an electric or a magnetic field. In the case of the electric-field–mediated interaction, the dipolar electric field of the exciton couples to longitudinal optical vibrations of the nuclei (LO phonons) through the Frohlich interaction (8). By measuring the QD emission intensity under appropriate optical resonance conditions, the optical phonon Raman spectrum of individual QDs can be measured. In the case of magnetic-field–mediated interactions, the exciton spin polarizes the nuclear spins within the QD through the contact hyperfine interaction (9). In return, the nuclear spins act back on the exciton and shift the exciton's energy (Overhauser shift). By measuring the magnitude of the Overhauser shift under nuclear magnetic resonance (NMR) conditions, it is possible to measure the NMR spectra of the nuclei within individual QDs.

We have studied semiconductor samples grown by molecular beam epitaxy containing layers of GaAs sandwiched between layers of $Al_xGa_{1-x}As$. The GaAs behaves like a quantum well for excitons. In thin GaAs layers (<100 nm), the energy resulting from spatial confinement is large, leading to significant changes in excitonic properties. Furthermore, because of atomic fluctuations at the interfaces, the excitons are also laterally confined (Fig. 1A). A one-monolayer change in the thickness of a 5-nm GaAs quantum well changes the exciton energy by about 10 meV, which is sufficient to completely localize the exciton at low temperature and provides an excellent model QD system for spectroscopic study (*1*–*5*). The NMR results were taken from a (001) $GaAs/Al_{0.3}Ga_{0.7}As$ sample with a GaAs well width of 15 monolayers and $Al_{0.3}Ga_{0.7}As$ barrier widths of 25 nm. Each monolayer includes an As and Ga layer and is 0.28 nm thick. This structure produced strong photoluminescence (PL) with narrow spectral linewidths. For the Raman scattering experiment, it was necessary to reduce the PL in order to measure the resonant Raman signal. For this purpose, we used thin AlAs barriers, which increased the tunneling rate out of the quantum well and reduced the PL intensity. A 19-monolayer GaAs quantum well sample with 5-nm barriers surrounded by 60-nm GaAs buffer layers was found to work well. Pure AlAs barriers were used to avoid $Al_xGa_{1-x}As$ alloy modes and simplify the phonon spectrum. In both samples, the lateral sizes of the QDs formed by the interface fluctuations are on the order of 10 to 100 nm (*2*, *4*).

The samples were excited by a Ti:sapphire laser with a power of about 50 W cm^{-2}, and the emitted light was detected in a backscattering geometry through a triple-grating spectrometer by a charge-coupled device detector with a resolution down to 30 μeV. Individual QDs were studied by exciting and detecting light through apertures ranging in diameter from 25 down to 0.2 μm in a metal mask patterned directly on the sample with electron-beam lithographic techniques (*2*). In this way, it is possible to spectroscopically study individual QDs with high sensitivity and spatial resolution (down into the optical near-field regime) (*2*–*5*). The sample was kept at a temperature of 6 K. For the NMR measurement, the sample was inserted into a longitudinal magnetic field of 1 T aligned normal to the quantum well. A four-turn Helmholtz coil provided a transverse radio-frequency magnetic field with an amplitude of about 0.7 G. The Raman experiments were performed with the polarization of the incident and detected light parallel to the same (110) crystal axis, whereas in the NMR experiments, the polarization of the incident and detected light was circular and linear, respectively.

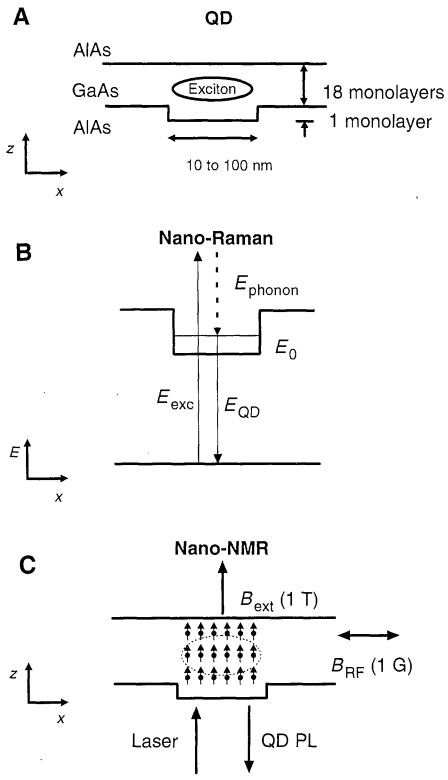

Fig. 1. (**A**) The QD's lateral localization within the GaAs/AlAs quantum well. (**B**) The resonant Raman process: The laser excites an exciton at energy E_{exc}, which can emit an optical phonon and reemit a photon at the QD energy. (**C**) The NMR experiment: Exciting the sample with circularly polarized laser light in the presence of a static magnetic field B_{ext} pumps the nuclear spins into a high state of polarization. The resonant transverse magnetic field B_{RF} destroys the nuclear polarization. The effect is measured through the magnitude of the Overhauser shift in the QD PL spectrum.

We first demonstrate the Raman spectroscopy of a single QD (Fig. 2). The PL spectrum from the GaAs/AlAs sample with an aperture size of 25 μm (Fig. 2A) provides an ensemble measurement of QDs, whereas the PL spectrum from a 0.8-μm aperture (Fig. 2C) shows a single QD PL line at E_0 (ground-state energy). An excitation spectrum in which the intensity of the QD PL

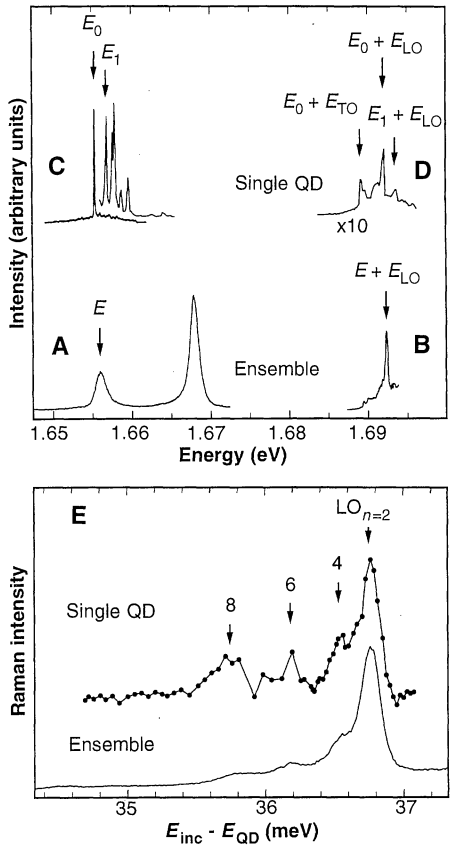

Fig. 2. GaAs/AlAs emission spectra demonstrating single QD Raman spectroscopy. (**A**) An ensemble PL measurement through a 25-μm aperture, showing emission at 1.656 and 1.668 eV from the 19- and 18-monolayer parts of the quantum well, respectively. (**B**) Ensemble PL excitation spectrum (25 μm). (**C** and **D**) PL and PL-excitation spectra, respectively, obtained through a 0.8-μm aperture. The PL spectrum shows a single-QD PL line at E_0. The excitation spectrum shows sharp electronic resonances within the first 10 meV and Raman resonances starting about 34 meV above the luminescing state. (**E**) The top spectrum is a high-resolution LO-phonon spectrum from a QD, obtained from the intensity of the QD emission as a function of the energy difference between the QD (E_{QD}) and the laser (E_{exc}) as the laser is scanned. The bottom (ensemble) spectrum is the resonant Raman spectrum obtained in the conventional way from the 25-μm aperture.

line at energy E_0 is plotted as a function of the laser energy (Fig. 2C) exhibits sharp resonances within about 10 meV of the QD PL line corresponding to direct absorption into QD states followed by relaxation into the luminescing state by emission of acoustic phonons (*2*). At higher energies (Fig. 2D), starting about one transverse optical (TO) phonon energy above the luminescing state, there is additional sharp structure, although about an order of magnitude weaker than the lower energy excitation resonances. This higher energy structure arises from absorption into two-dimensional (2D) exciton states, followed by a transition to the luminescing QD state accompanied by the emission of an optical phonon (Fig. 1B). The structure between the energies labeled $E_0 + E_{TO}$ and $E_0 + E_{LO}$ represents the optical phonon spectrum modulated by the QD exciton-phonon interaction. This strong enhancement corresponds to resonant Raman scattering from a single QD. The resonance linewidths are extremely sharp, allowing the selective probing of individual QDs through individual phonons. There is also a peak at higher energies ($E_1 + E_{LO}$) that corresponds to a two-step process in which the 2D exciton makes a transition into the excited state of the QD at E_1 accompanied by the emission of an LO phonon, and then makes a transition to the QD luminescing state by emitting an acoustic phonon.

The Raman spectrum from individual QDs can be acquired by plotting the intensity of that QD PL line as a function of the difference between the exciting and detected light energy ($E_{exc} - E_{QD}$) (Fig. 2E) for the LO_n phonon region. The structure in the ensemble spectrum (*10*) (bottom trace in Fig. 2E) is similar to previous studies (*11*) and arises from confined and interface LO phonons due to the vertical confinement as discussed previously (*8*, *12*). For example, LO_n arises from a confined phonon with an envelope function that has $n - 1$ nodes, and it goes to zero in the AlAs barriers. The LO_n phonons in single QD spectra (Fig. 2E) occur at the same energies as those measured in the ensemble spectrum with little fluctuation and with similar linewidths. This correspondence implies that the LO phonons are not confined in the lateral dimensions by the interface fluctuations, in sharp contrast to the excitons. Nevertheless, because the phonons are resonantly excited through the wave function of a single localized exciton, a localized phonon wave packet is excited, and only the nuclei within the QD are being probed. Interestingly, although the energies are the same, the relative intensities of the spectral features vary significantly. For example, the TO_2 phonon intensity relative to that of LO_2 becomes significantly stronger than the ensemble average in some cases (Fig. 2, B and D). This result likely arises from changes in the exciton-phonon scattering strength as the lateral shape and size of the QD varies, although we cannot rule out the possibility that the apertures lead to a z component of the electric field of the light that breaks the selection rules in some cases.

To probe the nuclear spins through magnetic resonance, it is necessary to apply a static longitudinal magnetic field (Fig. 1C). In this external field, the exciton spectral lines split into doublets as a result of the Zeeman interaction with the external field (*13*). However, there is also a contribution to the Zeeman splitting from the nuclear spin (*5*, *9*). This additional contribution can become strong under optical pumping with circularly polarized light in a sufficiently strong external field ($B_{ext} > 0.2$ T) (*14*). In the QDs, the nuclear spins can be optically pumped to polarization values in excess of 70% through the hyperfine interaction (*5*). This nuclear polarization acts back on the exciton and strongly enhances or reduces the Zeeman splitting, depending on the orientation of the polarization of the exciting light. This change in the Zeeman splitting, or Overhauser shift, can be described in terms of an internal effective magnetic field. We have measured internal effective fields as high as 1.5 T (*5*). The measurement of the Overhauser shift in the QD exciton's PL line provides a direct measure of the strength of the hyperfine interaction and the value of the nuclear polarization.

The nuclei can be strongly depolarized by applying a transverse magnetic field at radio frequencies (RF) that are resonant with the nuclear Zeeman splittings. The PL was first excited with σ_+ and σ_- polarized light (*15*) and with an applied longitudinal magnetic field of 1 T, but without the transverse resonant RF field (solid curves in Fig. 3A). With the σ_+ (σ_-) excitation, the Zeeman splitting was increased (decreased) by 90 μeV because of the optically pumped effective internal field. In a second measurement, the RF frequency was continuously swept over the Ga and As nuclear resonances with a sweep rate of 5 Hz as the PL was being measured (dashed curves in Fig. 3A). In this case, the nuclear contribution to the Zeeman splitting was strongly reduced, leading us to conclude that most of the nuclei are depolarized by the resonant RF field. This result verifies the nuclear origin of the enhanced Zeeman splitting and at the same time demonstrates the effectiveness of the depolarizing NMR field.

To demonstrate the NMR spectroscopy, the Zeeman splitting was measured as a function of the frequency of the transverse field as the RF was stepped through each of the nuclear resonances. In this way, single-QD ^{75}As and ^{69}Ga NMR spectra were recorded (Fig. 3, B and C, respectively). The relative strengths of the two NMR spectra can be understood in terms of the abundances of the nuclear isotopes and the nuclear gyromagnetic ratios (*9*). The resonant frequencies vary by tens of kilohertz between QDs, and some spectra are significantly broadened (up to a factor of 10). These effects illustrate the potential of NMR as a local probe. The capability of measuring changes in the Overhauser energy shift provides a direct and quantitative measure of the nuclear spin polarization that is not available if only the electronic polarization is monitored as in previous macroscopic studies using optical NMR (*16*).

The experiments described above were performed on single QDs that range in size from 3 to 6 nm in the vertical dimension and from about 10 to 100 nm in the lateral dimension. Such QDs consist of as few as 10^4 nuclei. These experiments are possible because of the high sensitivity of optical spectroscopy and because of the good selectivity possible with high-resolution detection and resonant excitation when the spectral lines are sharp. Nevertheless, these measurements remain challenging, and there are several conditions that we found to be important for success. In order to

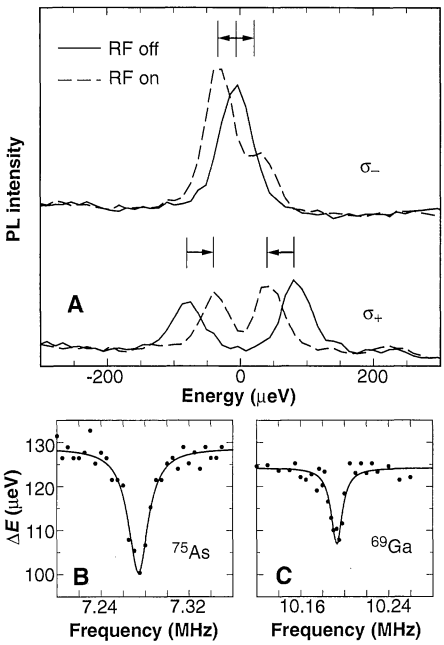

Fig. 3. (**A**) Zeeman splitting in a single QD PL spectral line centered at 1.6286 eV in a longitudinal magnetic field of B_{ext} = 1 T excited with either σ_+ or σ_- polarized light with (dashed lines) and without (solid lines) a transverse RF magnetic field continuously scanning through all the Ga and As nuclear magnetic resonances. (**B** and **C**) NMR spectra from another QD, showing the ^{75}As and ^{69}Ga resonances, respectively, at B_{ext} = 1 T.

measure the resonant Raman enhancement, it was necessary that the Raman intensities be at least comparable to the PL intensities. In the Raman sample, this condition was satisfied by using thin barriers to reduce the PL intensity. However, in other samples, such as the GaAs/$Al_{0.3}Ga_{0.7}As$ sample used for the NMR experiment, it was not possible to detect sufficient intensity enhancements on top of much stronger PL intensities, and we could not do Raman spectroscopy. In contrast to the Raman spectroscopy, the NMR was measured through changes in the PL energy. For this reason, the experiment benefits from a strongly luminescing sample. In both cases, the narrow spectral lines allowed us to resolve individual QDs, but in the NMR, because we were measuring changes in the Overhauser shifts, it was especially important to have very narrow PL spectral lines. Our spectral resolution (in other words, how well we can pick the resonance energy) is given roughly by the PL linewidth divided by the signal to noise ratio. Currently, this is about 5 μeV, and we can measure changes in nuclear polarization down to about 6%.

Previously, the most sensitive resonant Raman and optical NMR experiments performed on semiconductor nanostructures involved at least 10^9 nuclei (*11*, *16*). The current experiments represent an increase in sensitivity of five orders of magnitude. Recently, there has also been extensive effort in micro-Raman spectroscopy, including work at helium temperature (*17*), and there are pioneering efforts in optical-near-field Raman imaging at room temperature with lateral spatial resolutions down to 250 nm (*18*). It is important to note that, although the aperture sizes in our experiments were restricted to 200 nm or larger, the actual resolution of our experiments is much better because of our use of resonance techniques. By resonating with a single QD, we are probing the nuclei within that QD, and thus, our lateral spatial resolution is about 10 nm, an order of magnitude better than previous optical-near-field Raman spectroscopy. In some cases it should be possible to apply such resonance techniques to optical near-field imaging to enhance both sensitivity and selectivity.

There is no obvious reason why the experiments presented here could not be extended to smaller sizes or to other material systems. The present experiments demonstrate that if optical spectroscopy on single quantum units can be done, then nuclear spectroscopy on the same scale is possible.

REFERENCES AND NOTES

1. H. F. Hess, E. Betzig, T. D. Harris, L. N. Pfeiffer, K. W. West, *Science* **264**, 1740 (1994); K. Brunner, G. Abstreiter, G. Bohm, G. Trankle, G. Weimann, *Phys. Rev. Lett.* **73**, 1138 (1994); A. Zrenner *et al.*, *ibid.* **72**, 3382 (1994); W. Heller and U. Bockelmann, *Phys. Rev. B* **55**, R4871 (1997).
2. D. Gammon, E. S. Snow, D. S. Katzer, *Appl. Phys. Lett.* **67**, 2391 (1995).
3. D. Gammon, E. S. Snow, B. V. Shanabrook, D. S. Katzer, D. Park, *Science* **273**, 87 (1996).
4. _____ *Phys. Rev. Lett.* **76**, 3005 (1996).
5. S. W. Brown T. A. Kennedy, D. Gammon, E. S. Snow, *Phys. Rev B* **54**, R17339 (1996).
6. M. Nirmal *et al.*, *Nature* **383**, 802 (1996); S. A. Empedocles, D. J. Norris, M. G. Bawendi, *Phys. Rev. Lett.* **77**, 3873 (1996); S. A. Blanton, M. A. Hines, P. Guyot-Sionnest, *Appl. Phys. Lett.* **69**, 3905 (1996); Al. L. Efros and M. Rosen, *Phys. Rev. Lett.* **78**, 1110 (1997).
7. J. Kohler, A. C. J. Brouwer, E. J. J. Groenen, J. Schmidt, *Science* **268**, 1457 (1995); S. Nie and S. R. Emory, *ibid.* **275**, 1102 (1997); J. Wrachtrup, A. Gruber, L. Fleury, C. von Borczyskowski, *Chem. Phys. Lett.* **267**, 179 (1997).
8. For a review, see B. Jusserand and M. Cardona, in *Light Scattering in Solids V*, M. Cardona and G. Guntherodt, Eds. (Springer-Verlag, Heidelberg, 1989), pp. 49–152.
9. For a review, see D. Paget and V. L. Berkovits, in *Optical Orientation*, F. Meier and B. P. Zakharchenya, Eds. (North-Holland, New York, 1984), chap. 9.
10. We estimate 0.01 QDs μm^{-2} μeV^{-1} from the PL spectra at small apertures. This density gives about 300 QDs within the resonance linewidth in a 25-μm aperture.
11. D. Gammon, B. V. Shanabrook, D. S. Katzer, *Phys. Rev. Lett.* **67**, 1547 (1991).
12. There is convincing evidence that the structure at energies less than that of the LO_2 peak is primarily due to interface phonons mixed with confined phonons [A. J. Shields, M. P. Chamberlain, M. Cardona, K. Eberl, *Phys. Rev. B* **51**, 17728 (1995)].
13. The exciton is composed of an electron and a heavy hole, each of which has a spin degeneracy of 2. Of the four resulting combinations, only two are dipole-allowed and absorb or emit light. See, for example, H. W. van Kesteren, E. C. Cosman, W. A. J. A. van der Poel, C. T. Foxon, *Phys. Rev. B* **41**, 5283 (1990).
14. The longitudinal field must be larger than the dipole fields from neighboring nuclei (5 G) and large enough such that the magnetic Zeeman energy is greater than fine structure splitting arising from deviations from cylindrical symmetry (0.2 T) (*4*, *5*).
15. In the NMR measurements, the laser was tuned to the beginning of the 2D continuum about 10 meV above the QD spectral lines; therefore, a number of QDs were pumped simultaneously. The PL, however, probes individual QDs through the contact hyperfine interaction, which is a local interaction (*9*).
16. G. P. Flinn, R. T. Harley, M. J. Snelling, A. C. Tropper, T. M. Kerr, *Semicond. Sci. Technol.* **5**, 533 (1990); J. A. Marohn *et al.*, *Phys. Rev. Lett.* **75**, 1364 (1995); S. E. Barrett, R. Tycko, L. N. Pfeiffer, K. W. West, *ibid.* **72**, 1368 (1994); M. Krapf, G. Denninger, H. Pascher, G. Weimann, W. Schlapp, *Solid State Commun.* **78**, 459 (1991).
17. R. Hessmer *et al.*, *Phys. Rev. B* **46**, 4071 (1992).
18. C. L. Jahncke, M. A. Paesler, H. D. Hallen, *Appl. Phys. Lett.* **67**, 2483 (1995).

19. We gratefully acknowledge extended discussions with B. V. Shanabrook, Al. L. Efros, M. Rosen, and J. Yesinowski. This work was supported in part by the Office of Naval Research.

2 April 1997; accepted 15 May 1997

Identification of Maize Histone Deacetylase HD2 as an Acidic Nucleolar Phosphoprotein

Alexandra Lusser, Gerald Brosch, Adele Loidl, Hubertus Haas, Peter Loidl*

The steady state of histone acetylation is established and maintained by multiple histone acetyltransferases and deacetylases, and this steady state affects chromatin structure and function. The identification of a maize complementary DNA encoding the chromatin-bound deacetylase HD2 is reported. This protein was not homologous to the yeast *RPD3* transcriptional regulator. It was expressed throughout embryo germination in correlation with the proliferative activity of cells. Antibodies against recombinant HD2-p39 immunoprecipitated the native enzyme complex, which was composed of phosphorylated p39 subunits. Immunofluorescence microscopy and sequence homologies suggested nucleolar localization. HD2 is an acidic nucleolar phosphoprotein that might regulate ribosomal chromatin structure and function.

Posttranslational acetylation of ε-amino groups of lysines in the NH_2-terminal region of core histones has remained an enigmatic process for more than 30 years (*1*, *2*). The recent identification of histone acetyltransferase (HAT) and histone deacetylase (HD) genes as transcriptional regulators has increased our understanding of this postsynthetic modification (*3*–*9*). A mammalian HD was shown to be a homolog of the yeast *RPD3* (reduced potassium dependency) transcriptional regulator (*5*). In maize embryos, four biochemically distinct HDs have been characterized (*10*). We have recently purified maize HD2 (*11*), an enzyme with a molecular mass of about 400 kD; when denatured, HD2 splits into three polypeptides with molecular masses of 39 (p39), 42 (p42), and 45 kD (p45). Internal peptide sequences revealed that the three polypeptides are highly homologous (*11*). Oligonucleotides deduced from these sequences (Fig. 1) were used for amplification of the encoding cDNA by the reverse transcriptase–polymerase chain reaction (RT-PCR). Analysis of the complete cDNA [1121 base pairs (bp)] revealed an open reading frame

Department of Microbiology, University of Innsbruck Medical School, Fritz-Pregl-Str. 3, A-6020 Innsbruck, Austria.

*To whom correspondence should be addressed.